

- Rep* **8**, 504–509.
18. Schelbergen RF, Blom AB, van den Bosch MH, Sloetjes A, Abdollahi-Roodsaz S, Schreurs BW, Mort JS, Vogl T, Roth J, van den Berg WB and van Lent PL (2012) Alarmins S100A8 and S100A9 elicit a catabolic effect in human osteoarthritic chondrocytes that is dependent on Toll-like receptor 4. *Arthritis Rheum* **64**, 1477–1487.
  19. Smits P, Li P, Mandel J, Zhang Z, Deng JM, Behringer RR, de Crombrughe B and Lefebvre V (2001) The transcription factors L-Sox5 and Sox6 are essential for cartilage formation. *Dev Cell* **1**, 277–290.
  20. van Lent PL, Grevers L, Blom AB, Sloetjes A, Mort JS, Vogl T, Nacken W, van den Berg WB and Roth J (2008) Myeloid-related proteins S100A8/S100A9 regulate joint inflammation and cartilage destruction during antigen-induced arthritis. *Ann Rheum Dis* **67**, 1750–1758.
  21. Wagner T, Wirth J, Meyer J, Zabel B, Held M, Zimmer J, Pasantes J, Bricarelli FD, Keutel J, Hustert E, Wolf U, Tommerup N, Schempp W and Scherer G (1994) Autosomal sex reversal and campomelic dysplasia are caused by mutations in and around the SRY-related gene SOX9. *Cell* **79**, 1111–1120.
  22. Xiong Z, O'Hanlon D, Becker LE, Roder J, MacDonald JF and Marks A (2000) Enhanced calcium transients in glial cells in neonatal cerebellar cultures derived from S100B null mice. *Exp Cell Res* **257**, 281–289.
  23. Zreiqat H, Belluoccio D, Smith MM, Wilson R, Rowley LA, Jones K, Ramaswamy Y, Vogl T, Roth J, Bateman JF and Little CB (2010) S100A8 and S100A9 in experimental osteoarthritis. *Arthritis Res Ther* **12**, R16.

## Determination of differential gene expression profiles in superficial and deeper zones of mature rat articular cartilage using RNA sequencing of laser micro-dissected tissue specimens

Yoshifumi MORI<sup>1</sup>, Ung-il CHUNG<sup>2</sup>, Sakae TANAKA<sup>1</sup>, and Taku SAITO<sup>1,3</sup>

<sup>1</sup>Sensory & Motor System Medicine, <sup>2</sup>Center for Disease Biology and Integrative Medicine, Faculty of Medicine, <sup>3</sup>Bone and Cartilage Regenerative Medicine, University of Tokyo, 7-3-1 Hongo, Bunkyo-ku, Tokyo 113-8655, Japan

(Received 16 May 2014; and accepted 27 May 2014)

### ABSTRACT

Superficial zone (SFZ) cells, which are morphologically and functionally distinct from chondrocytes in deeper zones, play important roles in the maintenance of articular cartilage. Here, we established an easy and reliable method for performance of laser microdissection (LMD) on cryosections of mature rat articular cartilage using an adhesive membrane. We further examined gene expression profiles in the SFZ and the deeper zones of articular cartilage by performing RNA sequencing (RNA-seq). We validated sample collection methods, RNA amplification and the RNA-seq data using real-time RT-PCR. The combined data provide comprehensive information regarding genes specifically expressed in the SFZ or deeper zones, as well as a useful protocol for expression analysis of microsamples of hard tissues.

Osteoarthritis (OA), a chronic degenerative joint disorder characterized by articular cartilage destruction, is a major public health issue, causing pain and disability of the elderly worldwide (5, 8). Although effective disease-modifying treatments for OA have not been developed, its etiopathogenesis has been addressed in recent clinical studies. Cartilage degeneration is first observed at the articular surface in the form of fibrillation (24). Once the surface is disrupted, deeper cartilage layers are subsequently degraded (24).

Articular cartilage (AC) is composed of three layers: the superficial (SFZ), middle and deep zones. The SFZ, the outermost surface layer adjacent to the joint cavity, is histologically distinct from the deeper zones. In the SFZ, collagen fibers align parallel to the articular surface, in contrast to their vertical

alignment in the deeper layers (2, 17). SFZ cells, which also display parallel alignment, are smaller than chondrocytes in the deeper layers and exhibit characteristic flat morphology (10). SFZ cells produce lubricin, encoded by *Proteoglycan4* (*Prg4*), for surface lubrication. An homozygous mutant of the human *PRG4* gene causes the autosomal recessive camptodactyly-arthropathy-coxa vara-pericarditis syndrome that shows congenital or early-onset camptodactyly and childhood-onset noninflammatory arthropathy (1, 16). Mice lacking *Prg4* (*Prg4*<sup>-/-</sup>) exhibit early onset of osteoarthritis (25). In addition, chondrocytes obtained from SFZ display higher proliferative activity than those from deeper AC zones, implying that SFZ might be the main cell source of cartilage regeneration (32). Despite the potential roles of SFZ in the etiopathogenesis and pathophysiology of OA, apart from the involvement of Wnt/ $\beta$ -catenin signaling, TGF- $\beta$ /BMP signaling and high mobility group box 2 (HMGB2), molecular mechanisms regulating the differentiation and maintenance of SFZ are still unknown (12, 22, 28). This lack of data is mainly because comprehensive *in vivo* gene expression analysis of the SFZ is difficult due to its thinness, which makes it difficult to obtain SFZ-spe-

---

Address correspondence to: Taku Saito, M.D., Ph.D., Associate Professor  
Bone and Cartilage Regenerative Medicine, Faculty of Medicine, University of Tokyo, Hongo 7-3-1, Bunkyo-ku, Tokyo 113-8655, Japan  
Tel: +81-3-3815-5411 (ext. 37369), Fax: +81-3-3818-4082  
E-mail: tasaitou-tky@umin.ac.jp

cific samples.

To address this issue, we focused on a microsampling technique based on laser microdissection (LMD). LMD is an innovative technology that enables the isolation of a micro-area of tissue and has been widely used for a variety of biological research. Although LMD from a frozen sample is the ideal method for collection of RNA, preparation of a cryosection from hard tissue is difficult by conventional methods. In the present study, we aimed to establish an easy and reliable method for performance of LMD on cryosections of mature rat articular cartilage and for subsequent performance of RNA sequencing (RNA-seq) to obtain gene expression profiles for both the SFZ and deeper AC zones.

## MATERIALS AND METHODS

**Specimen preparation.** All animal experiments were undertaken according to the guidelines of the Animal Care and Use Committee of the University of Tokyo. Ten-week-old male Sprague Dawley rats (Sankyo Laboratories, Tokyo, Japan) were sacrificed by cervical dislocation under anesthesia. A ring-shaped skin incision was made at the height of the rib cage, the skin was dragged distally and the distal flap was inverted to expose the lower extremities. The left knee was then disarticulated, the medial and lateral menisci were detached and the tibia was cut at its shaft. The proximal tibia was immediately and directly placed into liquid nitrogen. Frozen sections were embedded in pre-cooled SCEM compound (Section-lab, Hiroshima, Japan) and stored at  $-80^{\circ}\text{C}$  until further analysis.

For H&E staining, 10- $\mu\text{m}$  paraffin-embedded sections were prepared from 10-week-old Sprague Dawley rats as described previously (18). H&E staining was performed according to a standard protocol.

**Laser microdissection (LMD).** We performed LMD using frozen sections prepared by Kawamoto's film method (11, 20). Specimens were placed into a Leica CM3050S (Leica Microsystems, Wetzlar, Germany) at  $-30^{\circ}\text{C}$  and cut coarsely in a frontal plane until a desired surface was exposed. The adhesive surface of Cryofilm Type IIC (Section-lab) was then attached to the specimen and 10- $\mu\text{m}$ -thick sections were cut. The specimen with attached film was fixed to a metal frame using a double-sided tape (Nichiban, Tokyo, Japan). This metal frame was prepared from a membrane slide (PEN-membrane, 2.0  $\mu\text{m}$ ) whose PEN-membrane was removed prior to use. The fixed specimen and attached film were stored in the gas

layer of liquid nitrogen until microdissection.

To prevent RNA degradation, frozen specimens (prior to thawing) were immediately soaked in 80% ethanol for 30 s, then in 100% ethanol for 1 min (twice), then in xylene for 5 min at room temperature and subsequently they were dried for 5 min. Specimens were then placed in a Leica LMD6500 (Leica Microsystems). Microdissection of the section was performed using the following settings: Power 50, Aperture 30 and Speed 5. Samples were collected in the cap of a 200  $\mu\text{L}$  tube pre-filled with 50  $\mu\text{L}$  of XB buffer of the Arcturus Picopure RNA isolation Kit (Thermo Fisher Scientific, Waltham, MA). SFZ and deeper AC samples from two slices were obtained for each rat. Samples were stored at  $-80^{\circ}\text{C}$  until mRNA extraction.

**RNA extraction and amplification.** RNA extraction was performed using the Picopure RNA isolation Kit according to the manufacturer's protocol. RNA was collected in 11  $\mu\text{L}$  of EB buffer, 1.5  $\mu\text{L}$  of which were then used for checking RNA purity using NanoDrop (Thermo Fisher Scientific). We then amplified the remaining sample by two rounds of *in-vitro* transcription using the Arcturus RiboAmp HS PLUS kit (Thermo Fisher Scientific) according to the manufacturer's protocol. Amplified RNA (aRNA) was obtained in 30  $\mu\text{L}$  of RNA elution buffer, 1.5  $\mu\text{L}$  of which were again analyzed using NanoDrop to check quantity and purity.

**Real-time RT-PCR.** One microgram of aRNA was reverse-transcribed using the QuantiTect Reverse-Transcription kit (Qiagen, Hilden, Germany) without performing the genomic DNA elimination reaction. The resultant 20  $\mu\text{L}$  of cDNA solution was diluted to 100  $\mu\text{L}$  with distilled water. For real-time RT-PCR analysis, the quantity of DNA polymerase was increased versus the standard protocol to rapidly amplify aRNAs with a small copy number (4). Reagents were prepared as follows: FastStart Universal SYBR Green Master (Roche Diagnostics, Basel, Switzerland) 10  $\mu\text{L}$ ; FastStart Taq DNA Polymerase (5 U/ $\mu\text{L}$ , Roche) 0.4  $\mu\text{L}$ ; forward Primer (10  $\mu\text{M}$ ) 2  $\mu\text{L}$ ; Reverse Primer (10  $\mu\text{M}$ ) 2  $\mu\text{L}$ ; distilled water 3.6  $\mu\text{L}$ , aRNA solution 2  $\mu\text{L}$ , and were run in triplicate on a Thermal Cycler Dice (Takara Bio, Otsu, Japan). Relative expression levels were calculated by the delta-delta CT method using *Gapdh* as an internal control. Primer pairs used are shown in Table 1.

**RNA sequencing (RNA-seq).** A cDNA library was constructed according to the TrueSeq RNA Sample

**Table 1** List of primers used for real-time RT-PCR

Gene	Forward primer	Reverse primer	Product size (bp)
<i>Gapdh</i>	TGCACCACCAACTGCTTAGC	GGATGCAGGGATGATGTTCT	177
<i>Col2a1</i>	ATGACTTTCCTCCGTCTACTGTCC	TGATGGTCTTGCCCCACTTAC	226
<i>Prg4</i>	AACCTGACTGGCAAAGAAGAATG	TGGGAGGAAGAGGAGGAATAAATAG	232
<i>Bmp7</i>	GCCCTTCCTTCCGTTCTATTT	CATCCCTCACCGACCTCTTC	129
<i>Tmem176a</i>	CGTCAGGCAGGAAGAAGACC	GGTGGTGAAGGCAGAGGAGA	117
<i>Wnt9a</i>	TGGCAGTGGACACACAAGG	TCGCCACACAGTTGAGGTAGA	80
<i>Frzb</i>	GGGAACCTCATGGTGCCTTTT	GGAATGAGACTTTTAGGTGATTGG	80
<i>Ibsp</i>	CAAACATGAATACACGGTGTGAG	TTATCTGTAGGGGAGGGGTTGT	93
<i>Grem1</i>	GATTATGCAGGCTATGACGGAAC	GCCAAATTAGCTTCTATGAGACCA	85

Preparation V2 Guide Rev. C (Illumina, San Diego, CA) and sequencing was performed using HiSeq 2000 (Illumina) according to the manufacturer's protocol. Then we normalized the sequence data by trimmed mean of M values method (26). The raw and processed data are available on GEO database with accession number GSE57377. After changing the measured value less than one to one, we calculated the fold change between SFZ and deeper AC.

*Statistical analysis.* Differences in mRNA expression levels between the SFZ and deeper AC as measured by real-time RT-PCR were analyzed using a paired *t*-test.

## RESULTS

### *Histological evaluation of articular cartilage*

In H&E-stained paraffin sections of the proximal tibia, the SFZ was easily distinguishable from deeper AC layers by its flat-shaped nuclei and its alignment parallel to the joint surface (Fig. 1A, left). The SFZ was also easily distinguishable without any staining in frozen sections on adhesive membrane (Fig. 1A, right). We therefore performed LMD on unstained sections.

### *LMD, RNA purification and amplification*

Both SFZ and deeper AC layers were easily cut and collected using LMD. We obtained a pair of SFZ and deeper AC samples from each of seven rats. After purification using the Picopure RNA isolation kit and amplification using the RiboAmp HS Plus kit, we ultimately obtained 4.1 to 28.0 µg aRNA from SFZ samples, and 4.0 to 74.6 µg from deeper AC samples.

### *Validation of accurate sampling by real-time RT-PCR*

After reverse-transcription of one µg aRNA, the accuracy of our sampling was validated by real-time RT-PCR. Previous studies showed that *Prg4* is up-regulated and *Col2a1* is downregulated in the SFZ compared to deeper AC (3, 21, 23, 25). Our real-time RT-PCR results showed significant upregulation of *Prg4* and downregulation of *Col2a1* in SFZ as compared to deeper AC, indicating that our differential sampling from these two distinct areas was appropriate (Fig. 1B).

### *RNA-seq*

RNA-seq was performed on two pairs of SFZ and deeper AC samples. Fold change in expression of a gene between SFZ and deeper AC was averaged for two pairs (rat 1 and rat 2), and genes with more than a 2-fold change (log<sub>2</sub>) on average were selected for further study. In total, 133 genes were found to be upregulated in SFZ and 758 genes were upregulated in deeper AC. The top 20 upregulated genes in SFZ and deeper AC are listed in Tables 2 and 3, respectively. Genes displaying lower fold changes are listed in Supplementary Tables S1 and S2, respectively. The present data showed upregulation of SFZ marker genes including *Wnt9a*, *Colla1*, *Errfi1*, *Clu*, *Thbs4*, *Igfbp5* and *Prg4* in the SFZ (9, 15, 21, 25, 27, 32), confirming that we appropriately collected RNA samples from SFZ and deeper AC.

### *Validation of RNA-seq results by real-time RT-PCR*

To confirm the reproducibility of the expression patterns obtained by RNA-seq, we analyzed the expression patterns of the three genes that displayed the highest fold change in the SFZ compared to deeper AC (*Bmp7*, *Tmem176a*, and *Wnt9a*) and those in deeper AC compared to the SFZ (*Frzb*, *Ibsp* and *Grem1*) using real-time RT-PCR. The expression

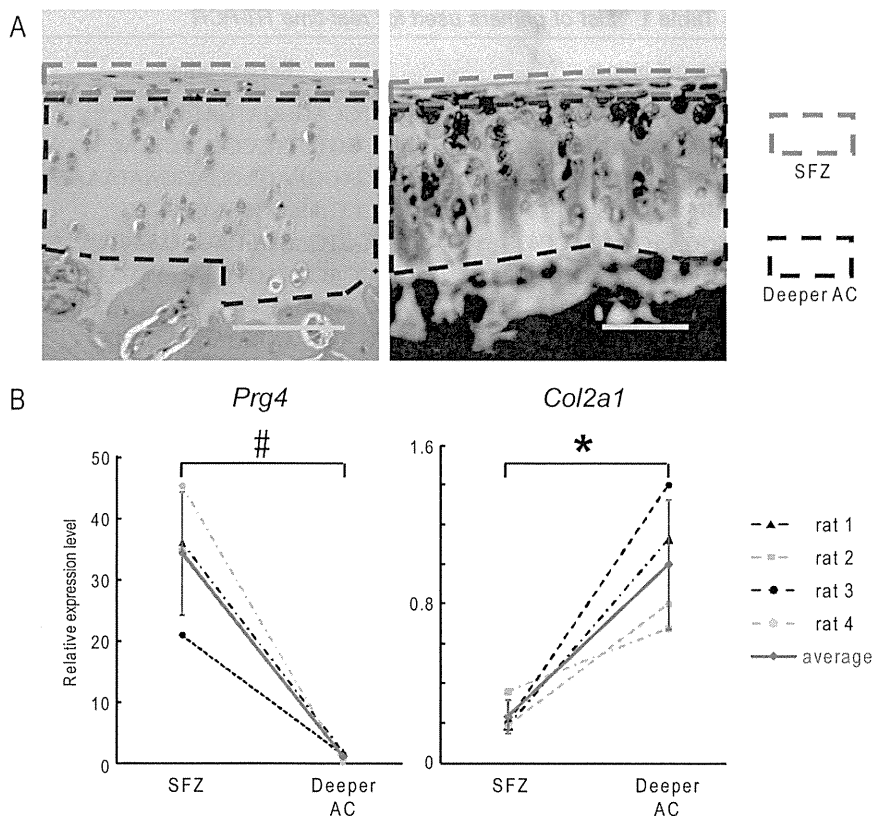


**Fig. 1** Microscopic and real-time RT-PCR analysis of articular cartilage zones and chondrocytes. **(A)** H&E staining of a paraffin-embedded section (left panel) and a frozen section on an adhesive membrane (right panel) of adult rat proximal tibia. Red and blue dashed line boxes indicate the superficial zone (SFZ) and deeper articular cartilage (AC), respectively. Scale bars, 100  $\mu$ m. **(B)** mRNA levels of *Prg4* and *Col2a1* in chondrocytes in the SFZ and deeper AC from four rats (rat 1 to 4), determined using real-time RT-PCR. All data are shown as means  $\pm$  SD. \* $P < 0.05$ , # $P < 0.005$ .

patterns of all six genes as determined by real-time RT-PCR were similar to those determined by RNA-seq (Fig. 2). Significant differences were observed in the mRNA levels of all genes except for *Bmp7* between the two zones, consistent with the results of the RNA-seq (Fig. 2).

## DISCUSSION

In the present study, we analyzed gene expression profiles of chondrocytes in the SFZ and deeper zones of mature rat articular cartilage using RNA-seq of laser microdissected tissue specimens. Since the articular cartilage is adjacent to the subchondral bone and the SFZ is extremely narrow, we had to optimize the conditions for all steps of protocol including preparation of a fine cryosection from hard tissue, specific dissection of SFZ, and reliable amplification of a small amount of RNA. Here, we established for the first time a successful procedure for examination of the RNA expression profile of a

micro-region of hard tissue using a combination of cryosectioning employing an adhesive membrane, LMD and RNA-seq.

Recent studies indicate that SFZ cells play essential roles in the homeostasis of articular cartilage (25, 27, 28, 32). The previous studies analyzed the expression of genes in SFZ by performing microarray analysis of SFZ cells isolated from neonatal mouse knee joints by digestion with trypsin and collagenase. However, the enzymatic treatment procedure might change the gene expression profile of SFZ from that *in vivo* (32). Since LMD is now the most commonly used commercially available micro-sampling procedure, we decided to use LMD for specific collection of SFZ cells. Although LMD has been widely used for sampling RNA, its application to a hard tissue such as bone has been rarely reported because of the difficulty of preparing fine cryosections of such tissue. Some previous studies reported LMD sampling of soft immature cartilage of rodent embryos or infants (31, 33). However, in our pre-

**Table 2** List of top 20 genes with higher expression in the SFZ than in deeper AC

Gene Symbol	Description	Fold Change (log2)
<i>Bmp7</i>	bone morphogenetic protein 7	51.5
<i>Tmem176a</i>	transmembrane protein 176A	45.3
<i>Wnt9a</i>	wingless-type MMTV integration site family, member 9A	32.7
<i>Gldc</i>	glycine dehydrogenase (decarboxylating)	26.5
<i>Mov10</i>	Moloney leukemia virus 10	24.5
<i>Prss23</i>	protease, serine, 23	23.6
<i>Cidea</i>	cell death-inducing DFFA-like effector a	23.4
<i>Cdh13</i>	cadherin 13	23.3
<i>Col1a1</i>	collagen, type I, alpha 1	22.7
<i>Kcnj8</i>	potassium inwardly-rectifying channel, subfamily J, member 8	20.7
<i>Slc8a1</i>	solute carrier family 8 (sodium/calcium exchanger), member 1	19.6
<i>Lrrc52</i>	leucine rich repeat containing 52	19.6
<i>Bend5</i>	BEN domain containing 5	18.8
<i>Sass6</i>	spindle assembly 6 homolog ( <i>C. elegans</i> )	18.4
<i>Kera</i>	keratocan	16.5
<i>Dact2</i>	dapper, antagonist of beta-catenin, homolog 2 ( <i>Xenopus laevis</i> )	16.5
<i>Cldn11</i>	claudin 11	16.3
<i>Pion</i>	pigeon homolog ( <i>Drosophila</i> )	13.6
<i>Htra4</i>	HtrA serine peptidase 4	13.3
<i>Arsi</i>	arylsulfatase family, member I	13.1

**Table 3** List of top 20 genes with higher expression in deeper AC than in the SFZ

Gene Symbol	Description	Fold Change (log2)
<i>Frzb</i>	frizzled-related protein	55.8
<i>Ibsp</i>	integrin-binding sialoprotein	45.9
<i>Grem1</i>	gremlin 1	45.5
<i>Rarres1</i>	retinoic acid receptor responder (tazarotene induced) 1	43.9
<i>Dmp1</i>	dentin matrix acidic phosphoprotein 1	40.9
<i>Tnni2</i>	troponin I type 2 (skeletal, fast)	38.7
<i>Gfap</i>	glial fibrillary acidic protein	35.0
<i>Arhgap18</i>	Rho GTPase activating protein 18	33.7
<i>F5</i>	coagulation factor V (proaccelerin, labile factor)	32.8
<i>Etnk2</i>	ethanolamine kinase 2	31.9
<i>Ogfr11</i>	opioid growth factor receptor-like 1	31.4
<i>R3hdml</i>	R3H domain (binds single-stranded nucleic acids) containing-like	28.6
<i>Mns1</i>	meiosis-specific nuclear structural 1	27.4
<i>Evi2a</i>	ecotropic viral integration site 2A	26.3
<i>Phospho1</i>	phosphatase, orphan 1	26.0
<i>Steap4</i>	STEAP family member 4	25.8
<i>Sptlc3</i>	serine palmitoyltransferase, long chain base subunit 3	23.8
<i>A2m</i>	alpha-2-macroglobulin	23.6
<i>Irx4</i>	iroquois homeobox 4	23.6
<i>Il17b</i>	interleukin 17B	23.2

liminary experiment, we were unable to make fine cryosections using the conventional methods due to subchondral bone beneath the articular cartilage. To overcome the difficulty, we adapted an unique cryosection method that uses an adhesive membrane to support the fine structure of the original tissue during the slicing procedure (11, 20). In addition to us-

ing the method, we also immediately dehydrated the sliced sections to facilitate the subsequent LMD. Using the modified cryosection method we efficiently obtained RNA from micro-areas of the fine cryosections.

Since only a small amount of RNA can be obtained using the LMD method, an amplification pro-

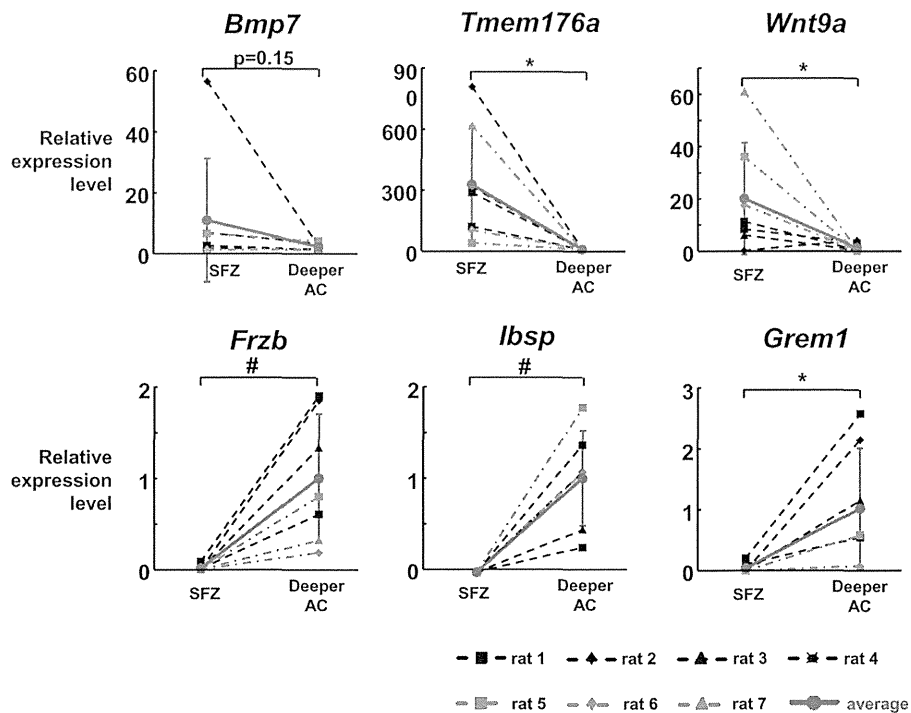


**Fig. 2** mRNA levels of the three genes with the highest fold change in the SFZ compared to deeper AC (*Bmp7*, *Tmem176a*, and *Wnt9a*) and those in deeper AC compared to the SFZ (*Frzb*, *Ibsp*, and *Grem1*), in cartilage of SFZ and deeper AC from seven rats (rat 1 to 7) determined by real-time RT-PCR. All data are shown as means  $\pm$  SD. \* $P < 0.05$ , # $P < 0.005$ .

cedure is indispensable for further gene expression analysis. Of several commercial amplification kits that we tested, the RiboAmp HS Plus kit provided the most reproducible results in quantification of representative marker genes by real-time RT-PCR. However, because this amplification system utilizes an *in vitro* transcription method, it can only amplify mRNA but not microRNA. Combination of our method with other novel methods should make it possible to further analyze other types of RNA or DNA in the future.

Microarray technology has been a standard method for comprehensive gene expression analysis for many years. Numerous data have been accumulated in previous studies using microarray analyses. However, microarray analysis has several limitations, including background noise, that arise from hybridization of cDNA samples and probes and also has an upper limit of signal strength (19, 30). On the other hand, gene quantification using RNA-seq is based on the number of sequences read, therefore upper or lower limits of signal strength do not exist. In addition, RNA-seq is free from mishybridization, a major cause of false positive signals in microarray analysis (19, 30).

In addition to previously reported marker genes

of the SFZ or deeper AC, the present data revealed distinct zone expression of several important molecules. Of the genes that were upregulated in the SFZ, *Bmp7* showed the highest fold change (Table 2), although significant difference was not observed in the mRNA levels of *Bmp7* between the two zones due to the high variability in its expression level in the SFZ (Fig. 2). *Bmp7* stimulates *Prg4* expression in articular cartilage explants and cultured articular chondrocytes (12, 22). Based on these results, *Bmp7* may function to stimulate production of ECM components in SFZ in a paracrine fashion. Of the genes that were upregulated in deeper AC, Wnt signaling antagonists including *Frzb*, *Grem1* and *Dkk1* were highly upregulated with an average fold change value of 55.77, 45.52 and 4.01, respectively (Table 3, Supplementary Table S2). Leijten *et al.* reported that these three genes are upregulated in articular cartilage compared to growth plate cartilage based on microarray analysis of samples from adolescent human donors (14). In long-bone explant organ culture and in human mesenchymal stem cell culture, treatment with these proteins suppressed hypertrophic differentiation without affecting chondrogenesis (14), indicating that these genes may direct immature chondrocytes to mature articular chondrocytes, not

to growth plate chondrocytes. Combined with our findings, the three genes may keep the character of articular chondrocytes in deeper zones from that of the SFZ cells or growth plate chondrocytes. Furthermore, Wnt/ $\beta$ -catenin signaling is activated in the SFZ and stimulates SFZ-cell proliferation and Prg4 production (13, 32). All of these findings support the idea that distinct regulation of Wnt/ $\beta$ -catenin signaling is essential for maintenance of the SFZ and deeper AC.

Fukui *et al.* previously performed microarray analysis of LMD samples obtained from the knee joint cartilage of OA patients (6, 7). They found that the gene expression patterns of chondrocytes differed according to the layer of articular cartilage in which they were situated, indicating that different phenotypes of articular chondrocytes in each layer may be essential for homeostasis of articular cartilage (6). In particular, the SFZ is indubitably the most potent layer for maintenance and repair of articular joints (25, 27, 28). Furthermore, studies of the rodent OA model have demonstrated many molecules and signaling pathways that play a role in the pathophysiology of OA (29). The present data provide useful knowledge that will contribute to the development of zone-specific Cre mice and to further determination of novel molecules that regulate SFZ cells.

In conclusion, we established a reliable technique that employs cryosections with an adhesive membrane, LMD and RNA-seq for analysis of gene expression profiles of hard tissue. By using this method, we demonstrated different gene expression profiles in the SFZ and the deeper layers of rat articular cartilage. The present RNA-seq data resource will contribute to OA research aimed at further understanding the functions of SFZ.

#### Acknowledgments

We thank J. Sugita, R. Yamaguchi and H. Kawahara for technical assistance. This study was supported by a Grant-in-aid for Scientific Research from the Japanese Ministry of Education, Culture, Sports, Science and Technology (#24390348).

#### REFERENCES

- Bahabri SA, Suwairi WM, Laxer RM, Polinkovsky A, Dalaan AA and Warman ML (1998) The camptodactyly-arthropathy-coxa vara-pericarditis syndrome: clinical features and genetic mapping to human chromosome 1. *Arthritis Rheum* **41**, 730–735.
- Clark JM (1990) The organisation of collagen fibrils in the superficial zones of articular cartilage. *J Anat* **171**, 117–130.
- Craig FM, Bentley G and Archer CW (1987) The spatial and temporal pattern of collagens I and II and keratan sulphate in the developing chick metatarsophalangeal joint. *Development* **99**, 383–391.
- Erickson HS, Albert PS, Gillespie JW, Rodriguez-Canale J, Marston Linehan W, Pinto PA, Chuaqui RF and Emmert-Buck MR (2009) Quantitative RT-PCR gene expression analysis of laser microdissected tissue samples. *Nat Protoc* **4**, 902–922.
- Felson DT and Zhang Y (1998) An update on the epidemiology of knee and hip osteoarthritis with a view to prevention. *Arthritis Rheum* **41**, 1343–1355.
- Fukui N, Ikeda Y, Ohnuki T, Tanaka N, Hikita A, Mitomi H, Mori T, Juji T, Katsuragawa Y, Yamamoto S, Sawabe M, Yamane S, Suzuki R, Sandell LJ and Ochi T (2008) Regional differences in chondrocyte metabolism in osteoarthritis: a detailed analysis by laser capture microdissection. *Arthritis Rheum* **58**, 154–163.
- Fukui N, Ikeda Y and Tanaka N (2011) The use of laser capture microdissection on adult human articular cartilage for gene expression analysis. *Methods Mol Biol* **755**, 449–459.
- Guccione AA, Felson DT, Anderson JJ, Anthony JM, Zhang Y, Wilson PW, Kelly-Hayes M, Wolf PA, Kreger BE and Kannel WB (1994) The effects of specific medical conditions on the functional limitations of elders in the Framingham Study. *Am J Public Health* **84**, 351–358.
- Hartmann C and Tabin CJ (2001) Wnt-14 plays a pivotal role in inducing synovial joint formation in the developing appendicular skeleton. *Cell* **104**, 341–351.
- Hughes LC, Archer CW and ap Gwynn I (2005) The ultrastructure of mouse articular cartilage: collagen orientation and implications for tissue functionality. A polarised light and scanning electron microscope study and review. *Eur Cell Mater* **9**, 68–84.
- Kawamoto T and Kawamoto K (2014) Preparation of thin frozen sections from nonfixed and undecalcified hard tissues using Kawamoto's film method (2012). *Methods Mol Biol* **1130**, 149–164.
- Khalafi A, Schmid TM, Neu C and Reddi AH (2007) Increased accumulation of superficial zone protein (SZP) in articular cartilage in response to bone morphogenetic protein-7 and growth factors. *J Orthop Res* **25**, 293–303.
- Koyama E, Shibukawa Y, Nagayama M, Sugito H, Young B, Yuasa T, Okabe T, Ochiai T, Kamiya N, Rountree RB, Kingsley DM, Iwamoto M, Enomoto-Iwamoto M and Pacifici M (2008) A distinct cohort of progenitor cells participates in synovial joint and articular cartilage formation during mouse limb skeletogenesis. *Dev Biol* **316**, 62–73.
- Leijten JC, Emons J, Sticht C, van Gool S, Decker E, Uitterlinden A, Rappold G, Hofman A, Rivadeneira F, Scherjon S, Wit JM, van Meurs J, van Blitterswijk CA and Karperien M (2012) Gremlin 1, frizzled-related protein, and Dkk-1 are key regulators of human articular cartilage homeostasis. *Arthritis Rheum* **64**, 3302–3312.
- Malda J, ten Hoope W, Schuurman W, van Osch GJ, van Weeren PR and Dhert WJ (2010) Localization of the potential zonal marker clusterin in native cartilage and in tissue-engineered constructs. *Tissue Eng Part A* **16**, 897–904.
- Marcelino J, Carpten JD, Suwairi WM, Gutierrez OM, Schwartz S, Robbins C, Sood R, Makalowska I, Baxevasis A, Johnstone B, Laxer RM, Zemel L, Kim CA, Herd JK, Ihle J, Williams C, Johnson M, Raman V, Alonso LG, Brunoni D, Gerstein A, Papadopoulos N, Bahabri SA, Trent JM and Warman ML (1999) CACP, encoding a secreted proteoglycan, is mutated in camptodactyly-arthropathy-coxa vara-peri-



- carditis syndrome. *Nat Genet* **23**, 319–322.
17. Minns RJ and Steven FS (1977) The collagen fibril organization in human articular cartilage. *J Anat* **123**, 437–457.
  18. Mori Y, Saito T, Chang SH, Kobayashi H, Ladel CH, Guehring H, Chung UI and Kawaguchi H (2014) Identification of fibroblast growth factor-18 as a molecule to protect adult articular cartilage by gene expression profiling. *J Biol Chem* **289**, 10192–10200.
  19. Nagalakshmi U, Wang Z, Waern K, Shou C, Raha D, Gerstein M and Snyder M (2008) The transcriptional landscape of the yeast genome defined by RNA sequencing. *Science* **320**, 1344–1349.
  20. Nakamura Y, Nomura Y, Arai C, Noda K, Oikawa T, Kogure K, Kawamoto T and Hanada N (2007) Laser capture microdissection of rat periodontal ligament for gene analysis. *Bio-tech Histochem* **82**, 295–300.
  21. Nalin AM, Greenlee TK Jr. and Sandell LJ (1995) Collagen gene expression during development of avian synovial joints: transient expression of types II and XI collagen genes in the joint capsule. *Dev Dyn* **203**, 352–362.
  22. Niikura T and Reddi AH (2007) Differential regulation of lubricin/superficial zone protein by transforming growth factor beta/bone morphogenetic protein superfamily members in articular chondrocytes and synoviocytes. *Arthritis Rheum* **56**, 2312–2321.
  23. Pacifici M, Koyama E and Iwamoto M (2005) Mechanisms of synovial joint and articular cartilage formation: recent advances, but many lingering mysteries. *Birth Defects Res C Embryo Today* **75**, 237–248.
  24. Poole AR, Guilak F and Abramson SB (2007) Etiopathogenesis of osteoarthritis. In: *Osteoarthritis*. (Moskowitz RW, Altman RD, Hochberg MC, Buckwalter JA and Goldberg VM, eds.) pp 27–49, Wolters Kluwer, Philadelphia.
  25. Rhee DK, Marcelino J, Baker M, Gong Y, Smits P, Lefebvre V, Jay GD, Stewart M, Wang H, Warman ML and Carpten JD (2005) The secreted glycoprotein lubricin protects cartilage surfaces and inhibits synovial cell overgrowth. *J Clin Invest* **115**, 622–631.
  26. Robinson MD and Oshlack A (2010) A scaling normalization method for differential expression analysis of RNA-seq data. *Genome Biol* **11**, R25.
  27. Staal B, Williams BO, Beier F, Vande Woude GF and Zhang YW (2014) Cartilage-specific deletion of Mig-6 results in osteoarthritis-like disorder with excessive articular chondrocyte proliferation. *Proc Natl Acad Sci USA* **111**, 2590–2595.
  28. Taniguchi N, Carames B, Kawakami Y, Amendt BA, Komiya S and Lotz M (2009) Chromatin protein HMGB2 regulates articular cartilage surface maintenance via beta-catenin pathway. *Proc Natl Acad Sci USA* **106**, 16817–16822.
  29. Wang M, Shen J, Jin H, Im HJ, Sandy J and Chen D (2011) Recent progress in understanding molecular mechanisms of cartilage degeneration during osteoarthritis. *Ann N Y Acad Sci* **1240**, 61–69.
  30. Wang Z, Gerstein M and Snyder M (2009) RNA-Seq: a revolutionary tool for transcriptomics. *Nat Rev Genet* **10**, 57–63.
  31. Yamane S, Cheng E, You Z and Reddi AH (2007) Gene expression profiling of mouse articular and growth plate cartilage. *Tissue Eng* **13**, 2163–2173.
  32. Yasuhara R, Ohta Y, Yuasa T, Kondo N, Hoang T, Addya S, Fortina P, Pacifici M, Iwamoto M and Enomoto-Iwamoto M (2011) Roles of beta-catenin signaling in phenotypic expression and proliferation of articular cartilage superficial zone cells. *Lab Invest* **91**, 1739–1752.
  33. Zhang M, Pritchard MR, Middleton FA, Horton JA and Damron TA (2008) Microarray analysis of perichondral and reserve growth plate zones identifies differential gene expressions and signal pathways. *Bone* **43**, 511–520.

**Supplementary Table S1** *List of genes with higher expression in the SFZ than in Deeper AC (ranks lower than 20th, fold change (log2) > 2)*

Gene Symbol	Description	Fold Change (log2)
Gp1bb	glycoprotein 1b (platelet), beta polypeptide	12.7
Ttll12	tubulin tyrosine ligase-like family, member 12	12.7
Aifm3	apoptosis-inducing factor, mitochondrion-associated 3	12.3
Il15	interleukin 15	10.7
Cd74	Cd74 molecule, major histocompatibility complex, class II invariant chain	10.6
Aldh1a2	aldehyde dehydrogenase 1 family, member A2	10.6
Tcp11	t-complex protein 11	10.3
Myoc	myocilin	10.0
Fbxo43	F-box protein 43	9.3
MARCH8	retinoblastoma-like 1 (p107)	9.1
Tead1	TEA domain family member 1	8.3
Rph3al	rabphilin 3A-like (without C2 domains)	8.2
Rxrg	retinoid X receptor gamma	8.2
Errfi1	ERBB receptor feedback inhibitor 1	8.0
Ntrk3	neurotrophic tyrosine kinase, receptor, type 3	7.9
Slc2a9	solute carrier family 2 (facilitated glucose transporter), member 9	7.6
Mfsd6	major facilitator superfamily domain containing 6	7.6
Nudt6	nudix (nucleoside diphosphate linked moiety X)-type motif 6	7.2
Tmprss2	transmembrane protease, serine 2	7.0
Clu	clusterin	6.5
Hs3st1	heparan sulfate (glucosamine) 3-O-sulfotransferase 1	6.5
RGD1311164	similar to DNA segment, Chr 6, Wayne State University 163, expressed	6.2
Thbs4	thrombospondin 4	6.2
Bmp4	bone morphogenetic protein 4	6.1
Arhgdib	Rho, GDP dissociation inhibitor (GDI) beta	5.5
Hbegf	heparin-binding EGF-like growth factor	5.5
Casr	calcium-sensing receptor	5.5
Mgl1	monoglyceride lipase	5.3
Zc3h3	zinc finger CCCH type containing 3	5.2
Rnf208	ring finger protein 208	5.2
Prrx1	paired related homeobox 1	5.2
Adhfe1	alcohol dehydrogenase, iron containing, 1	5.1
Egfl6	EGF-like-domain, multiple 6	5.0
Igfbp5	insulin-like growth factor binding protein 5	5.0
Sema4b	Semaphorin 4B	4.9
RGD1309708	similar to RIKEN cDNA 4930455F23	4.9
Cxcl12	chemokine (C-X-C motif) ligand 12	4.7
Slc6a12	solute carrier family 6 (neurotransmitter transporter, betaine/GABA), member 12	4.6
Cdh23	cadherin 23 (otocadherin)	4.4
Ncald	neurocalcin delta	4.4

**Supplementary Table S1** (continued)

Gene Symbol	Description	Fold Change (log2)
Itih3	inter-alpha trypsin inhibitor, heavy chain 3	4.4
Gch1	GTP cyclohydrolase 1	4.3
Pnpla2	patatin-like phospholipase domain containing 2	4.3
Scara3	scavenger receptor class A, member 3	4.1
Sectm1b	secreted and transmembrane 1B	4.1
Ifi2712b	interferon, alpha-inducible protein 27 like 2B	4.1
Tll1	tolloid-like 1	3.9
Bik	BCL2-interacting killer (apoptosis-inducing)	3.9
Tc2n	tandem C2 domains, nuclear	3.9
Nkx6-1	NK6 homeobox 1	3.9
Scg5	secretogranin V	3.9
Lhfp12	lipoma HMGIC fusion partner-like 2	3.9
Cdon	Cdon homolog (mouse)	3.8
Fhdc1	FH2 domain containing 1	3.7
Sult2b1	sulfotransferase family, cytosolic, 2B, member 1	3.6
Msx1	msh homeobox 1	3.6
Ampd3	adenosine monophosphate deaminase 3	3.6
Wnt11	wingless-type MMTV integration site family, member 11	3.5
Rarres2	retinoic acid receptor responder (tazarotene induced) 2	3.5
Clic2	chloride intracellular channel 2	3.5
Mfsd2a	major facilitator superfamily domain containing 2A	3.5
Gda	guanine deaminase	3.5
Plekhb1	pleckstrin homology domain containing, family B (evectins) member 1	3.3
Mgp	matrix Gla protein	3.2
Egln3	EGL nine homolog 3 (C. elegans)	3.2
Ppap2b	phosphatidic acid phosphatase type 2B	3.2
Xrcc2	X-ray repair complementing defective repair in Chinese hamster cells 2	3.1
Pigl	phosphatidylinositol glycan anchor biosynthesis, class L	3.1
Nrk	Nik related kinase	3.1
Hmcn1	hemicentin 1	3.1
MGC105649	hypothetical LOC302884	3.1
Slc40a1	solute carrier family 39 (iron-regulated transporter), member 1	3.0
Tspan13	tetraspanin 13	3.0
Optc	opticin	3.0
Sec31b	SEC31 homolog B (S. cerevisiae)	3.0
Wdfy2	WD repeat and FYVE domain containing 2	3.0
Rin2	Ras and Rab interactor 2	2.9
Dagla	diacylglycerol lipase, alpha	2.9
Jup	junction plakoglobin	2.8
Rem1	RAS (RAD and GEM)-like GTP-binding 1	2.8
Cstf3	cleavage stimulation factor, 3' pre-RNA, subunit 3	2.8
Clock	clock homolog (mouse)	2.7
Mylk	myosin light chain kinase	2.7
Crip1	cysteine-rich protein 1 (intestinal)	2.7
Plxdc2	plexin domain containing 2	2.7
Zmym1	zinc finger, MYM-type 1	2.7
Ptgs1	prostaglandin-endoperoxide synthase 1	2.7
ErbB3	v-erb-b2 erythroblastic leukemia viral oncogene homolog 3 (avian)	2.7
Pla1a	phospholipase A1 member A	2.6
Ptpn21	protein tyrosine phosphatase, non-receptor type 21	2.6

**Supplementary Table S1** (continued)

Gene Symbol	Description	Fold Change (log2)
Hipk4	homeodomain interacting protein kinase 4	2.6
Ltbp2	latent transforming growth factor beta binding protein 2	2.6
Ltbp4	latent transforming growth factor beta binding protein 4	2.6
Sulf1	sulfatase 1	2.6
Prg4	proteoglycan 4	2.6
Ano6	anoctamin 6	2.6
Fam163a	family with sequence similarity 163, member A	2.5
Cpne9	copine family member IX	2.5
Zfp709l2	zinc finger protein 709-like 2	2.5
Arhgef19	Rho guanine nucleotide exchange factor (GEF) 19	2.5
Sema3b	Semaphorin 3B	2.5
Tnfrsf9	tumor necrosis factor receptor superfamily, member 9	2.5
Gem	GTP binding protein (gene overexpressed in skeletal muscle)	2.5
Zfp775	zinc finger protein 775	2.5
Zbtb45	zinc finger and BTB domain containing 45	2.4
Rcan1	regulator of calcineurin 1	2.4
Got1	glutamic-oxaloacetic transaminase 1, soluble (aspartate aminotransferase 1)	2.3
Def6	differentially expressed in FDCP 6 homolog (mouse)	2.3
Vps13a	vacuolar protein sorting 13 homolog A (S. cerevisiae)	2.2
Des	desmin	2.2
Osbp2	oxysterol binding protein 2	2.2
Vstm4	V-set and transmembrane domain containing 4	2.2
Crtc2	CREB regulated transcription coactivator 2	2.2

**Supplementary Table S2** *List of genes with higher expression in Deeper AC than in the SFZ (ranks lower than 20th, fold change (log2) > 2)*

Gene Symbol	Description	Fold Change (log2)
Olr397	olfactory receptor 397	22.8
Alpl	alkaline phosphatase, liver/bone/kidney	22.5
Batf	basic leucine zipper transcription factor, ATF-like	22.4
Cks2	CDC28 protein kinase regulatory subunit 2	22.4
Tas2r120	taste receptor, type 2, member 120	22.1
Timp4	tissue inhibitor of metalloproteinase 4	22.0
Lysmd3	LysM, putative peptidoglycan-binding, domain containing 3	21.3
Mmp23	matrix metalloproteinase 23	20.1
Gmip	Gem-interacting protein	19.8
Klhl38	kelch-like 38 (Drosophila)	19.5
Foxa2	forkhead box A2	19.4
Fam111a	family with sequence similarity 111, member A	19.3
Zfp507	zinc finger protein 507	19.2
Tecta	tectorin alpha	19.2
Adam411	a disintegrin and metalloproteinase domain 4-like 1	19.0
Kcna1	potassium voltage-gated channel, shaker-related subfamily, member 1	18.6
Tsga13	testis specific, 13	18.5
Ivns1abp	influenza virus NS1A binding protein	18.2
Amhr2	anti-Mullerian hormone receptor, type II	17.7
Nsdhl	NAD(P) dependent steroid dehydrogenase-like	17.7
Mmp13	matrix metalloproteinase 13	17.4
Sox13	SRY (sex determining region Y)-box 13	17.3
Kcnk1	potassium channel, subfamily K, member 1	17.1
Slc6a1	solute carrier family 6 (neurotransmitter transporter, GABA), member 1	17.1
Ssx2ip	synovial sarcoma, X breakpoint 2 interacting protein	17.1
Dnm3	dynamamin 3	17.1
SEPT1	NudC domain containing 1	16.9
Hsd17b13	hydroxysteroid (17-beta) dehydrogenase 13	16.9
Akr1c19	aldo-keto reductase family 1, member C19	16.9
Tpbp	trophoblast glycoprotein	16.6
Syt8	synaptotagmin VIII	16.5
Sphk1	sphingosine kinase 1	16.4
Odz3	odz, odd Oz/ten-m homolog 3 (Drosophila)	16.2
Kcnk6	potassium channel, subfamily K, member 6	15.9
Csrp2	cysteine and glycine-rich protein 2	15.9
Hoxa13	homeo box A13	15.6
Echdc2	enoyl CoA hydratase domain containing 2	15.5
Pcdha5	protocadherin alpha 5	15.3
SEPT11	hyaluronan and proteoglycan link protein 4	15.0
Rhbdl2	rhomboid, veinlet-like 2 (Drosophila)	15.0

## Gene expression in cartilage

**Supplementary Table S2** (continued)

Gene Symbol	Description	Fold Change (log2)
Chd1	chromodomain helicase DNA binding protein 1	15.0
Tfr2	transferrin receptor 2	14.8
Abhd3	abhydrolase domain containing 3	14.7
LOC100125362	hypothetical protein LOC100125362	14.6
Vcpip1	valosin containing protein (p97)/p47 complex interacting protein 1	14.6
RGD1306941	similar to CG31122-PA	14.4
Art3	ADP-ribosyltransferase 3	14.3
Slc19a2	solute carrier family 19 (thiamine transporter), member 2	14.3
Mcc	mutated in colorectal cancers	14.1
Hadh	hydroxyacyl-CoA dehydrogenase	14.1
Mybph	myosin binding protein H	14.1
Tmem132e	transmembrane protein 132E	14.1
Wwtr1	WW domain containing transcription regulator 1	13.9
Cdv3	carnitine deficiency-associated gene expressed in ventricle 3 homolog (mouse)	13.8
Dact3	dapper, antagonist of beta-catenin, homolog 3 ( <i>Xenopus laevis</i> )	13.7
Slc10a7	solute carrier family 10, member 7	13.6
Eln	elastin	13.6
Fkbp1	FK506 binding protein-like	13.5
LOC688390	hypothetical protein LOC688390	13.4
Gstt1	glutathione S-transferase theta 1	13.4
Myom1	myomesin 1	13.4
Wdr53	WD repeat domain 53	13.3
Preli2	PRELI domain containing 2	13.2
Ppp1r14c	protein phosphatase 1, regulatory (inhibitor) subunit 14c	13.1
Fam70b	family with sequence similarity 70, member B	13.1
Plk5	polo-like kinase 5	13.0
Pcdh18	protocadherin 18	12.9
Wasf2	WAS protein family, member 2	12.9
Tfpi	tissue factor pathway inhibitor	12.8
Irf5	interferon regulatory factor 5	12.8
Kcnk2	potassium channel, subfamily K, member 2	12.7
Fmo4	flavin containing monooxygenase 4	12.5
Olr1014	olfactory receptor 1014	12.4
Ndr4	N-myc downstream regulated gene 4	12.4
Arhgdig	Rho GDP dissociation inhibitor (GDI) gamma	12.1
Pnkp	polynucleotide kinase 3'-phosphatase	12.1
Fgfr3	fibroblast growth factor receptor 3	12.0
Masp1	mannan-binding lectin serine peptidase 1	12.0
Mtpn	myotrophin	12.0
Anpep	alanyl (membrane) aminopeptidase	12.0
Parva	parvin, alpha	11.9
Fbp1	fructose-1,6-bisphosphatase 1	11.9
LOC688459	hypothetical protein LOC688459	11.9
Zfp689	zinc finger protein 689	11.8
Rnase10	ribonuclease, RNase A family, 10 (non-active)	11.7
Pdpr	pyruvate dehydrogenase phosphatase regulatory subunit	11.7
Igf1r1	IGF-like family receptor 1	11.7
Ina	internexin neuronal intermediate filament protein, alpha	11.7
Ccrn4l	CCR4 carbon catabolite repression 4-like ( <i>S. cerevisiae</i> )	11.4
Serinc2	serine incorporator 2	11.4

**Supplementary Table S2** (continued)

Gene Symbol	Description	Fold Change (log2)
Nat1	N-acetyltransferase 1	11.4
SEPT5	PYD and CARD domain containing	11.3
Gpr22	G protein-coupled receptor 22	11.2
Snrnp70	small nuclear ribonucleoprotein 70 (U1)	11.2
Tbccd1	TBCC domain containing 1	11.2
Dnah1	dynein, axonemal, heavy chain 1	11.2
RGD1565983	similar to apurinic/apyrimidinic endonuclease 2	11.1
Kctd4	potassium channel tetramerisation domain containing 4	11.1
Gpr171	G protein-coupled receptor 171	11.0
Zfp444	zinc finger protein 444	10.9
Pik3cb	phosphoinositide-3-kinase, catalytic, beta polypeptide	10.9
Hlx	H2.0-like homeobox	10.9
Nrsn2	neurensin 2	10.9
Pgm3	phosphoglucomutase 3	10.8
Lcmt2	leucine carboxyl methyltransferase 2	10.8
Trim43a	tripartite motif-containing 43A	10.8
Klf11	Kruppel-like factor 11	10.8
Eid3	EP300 interacting inhibitor of differentiation 3	10.8
RGD1562673	similar to Prostatic spermine-binding protein precursor (SBP)	10.8
Cd248	CD248 molecule, endosialin	10.7
Capn3	calpain 3	10.7
MARCH1	kelch-like 25 (Drosophila)	10.7
SEPT7	calreticulin 3	10.6
S1pr5	sphingosine-1-phosphate receptor 5	10.6
Rrad	Ras-related associated with diabetes	10.6
Vill	villin-like	10.6
Fads1	fatty acid desaturase 1	10.6
Irf6	interferon regulatory factor 6	10.5
Dync11l1	dynein cytoplasmic 1 light intermediate chain 1	10.4
Skap2	src kinase associated phosphoprotein 2	10.4
Cd2ap	CD2-associated protein	10.4
Clip2	CAP-GLY domain containing linker protein 2	10.4
Pglyrp1	peptidoglycan recognition protein 1	10.3
Bcas1	breast carcinoma amplified sequence 1	10.2
Fam117a	family with sequence similarity 117, member A	10.2
Cntf	ciliary neurotrophic factor	10.2
Paox	polyamine oxidase (exo-N4-amino)	10.2
Nagpa	N-acetylglucosamine-1-phosphodiester alpha-N-acetylglucosaminidase	10.2
C2	complement component 2	10.2
RGD1312026	similar to RIKEN cDNA C230081A13	10.1
Tuft1	tuftelin 1	10.1
Acbd5	acyl-CoA binding domain containing 5	10.1
Arhgap24	Rho GTPase activating protein 24	10.0
Myo1e	myosin IE	9.9
Slc22a18	solute carrier family 22, member 18	9.9
Gpr68	G protein-coupled receptor 68	9.8
Abhd10	abhydrolase domain containing 10	9.7
Il17re	interleukin 17 receptor E	9.7
Tfdp2	transcription factor Dp-2 (E2F dimerization partner 2)	9.7
Zfp800	zinc finger protein 800	9.7

**Supplementary Table S2** (continued)

Gene Symbol	Description	Fold Change (log2)
Fgfr1	Fibroblast growth factor receptor 1	9.6
Slc29a2	solute carrier family 29 (nucleoside transporters), member 2	9.6
MARCH4	DnaJ (Hsp40) homolog, subfamily C, member 5 gamma	9.6
Pcdha13	protocadherin alpha 13	9.5
Taok1	TAO kinase 1	9.5
Prmt7	protein arginine methyltransferase 7	9.5
Cpeb4	cytoplasmic polyadenylation element binding protein 4	9.5
Pof1b	premature ovarian failure 1B	9.4
MARCH7	major facilitator superfamily domain containing 9	9.4
Crlf1	cytokine receptor-like factor 1	9.3
Pole2	polymerase (DNA directed), epsilon 2 (p59 subunit)	9.3
Ankrd23	ankyrin repeat domain 23	9.3
RGD1359634	similar to RIKEN cDNA 1700088E04	9.2
Mms22l	MMS22-like, DNA repair protein	9.1
Ppm1l	protein phosphatase, Mg <sup>2+</sup> /Mn <sup>2+</sup> dependent, 1L	9.1
Sh3bp2	SH3-domain binding protein 2	9.1
SEPT3	ferredoxin-fold anticodon binding domain containing 1	9.0
Spata2L	spermatogenesis associated 2-like	9.0
Mal	mal, T-cell differentiation protein	8.9
Matn3	matrilin 3	8.9
Zfp583	zinc finger protein 583	8.9
Letm2	leucine zipper-EF-hand containing transmembrane protein 2	8.9
Cdk1	cyclin-dependent kinase 1	8.8
Aspg	asparaginase homolog (S. cerevisiae)	8.8
Zhx3	zinc fingers and homeoboxes 3	8.8
Iqgap3	IQ motif containing GTPase activating protein 3	8.8
Gpr116	G protein-coupled receptor 116	8.7
Lrp4	low density lipoprotein receptor-related protein 4	8.7
Mug1	murinoglobulin 1	8.7
Mum11l	melanoma associated antigen (mutated) 1-like 1	8.7
Zap70	zeta-chain (TCR) associated protein kinase	8.7
Tmie	transmembrane inner ear	8.7
Sorcs2	sortilin-related VPS10 domain containing receptor 2	8.7
Scgb1c1	secretoglobin, family 1C, member 1	8.6
Pdlim3	PDZ and LIM domain 3	8.6
Zfp112	zinc finger protein 112	8.5
Slc13a5	solute carrier family 13, member 5	8.5
Slk	STE20-like kinase (yeast)	8.5
Olr584	olfactory receptor 584	8.4
Shbg	sex hormone binding globulin	8.4
Slc12a1	solute carrier family 12, member 1	8.4
Mettl4	methyltransferase like 4	8.4
Fam13a	family with sequence similarity 13, member A	8.3
Fem1b	fem-1 homolog b (C. elegans)	8.3
Prkg2	protein kinase, cGMP-dependent, type II	8.3
Shq1	SHQ1 homolog (S. cerevisiae)	8.2
Cdc7	cell division cycle 7 homolog (S. cerevisiae)	8.2
Slc16a10	solute carrier family 16, member 10	8.2
Mecom	MDS1 and EVI1 complex locus	8.1
Bdh1	3-hydroxybutyrate dehydrogenase, type 1	8.1



**Supplementary Table S2** (continued)

Gene Symbol	Description	Fold Change (log2)
Gap43	growth associated protein 43	8.1
Cpamd8	C3 and PZP-like, alpha-2-macroglobulin domain containing 8	8.1
Rnf11	ring finger protein 11	8.0
Kif12	kinesin family member 12	8.0
Slc4a8	solute carrier family 4, sodium bicarbonate cotransporter, member 8	8.0
Rhobtb2	Rho-related BTB domain containing 2	8.0
Ren	renin	8.0
Fpgt	fucose-1-phosphate guanylyltransferase	8.0
Slc25a45	solute carrier family 25, member 45	8.0
Olr1229	olfactory receptor 1229	7.9
Apc2	adenomatous polyposis coli 2	7.9
Ing5	inhibitor of growth family, member 5	7.9
Cnksr1	connector enhancer of kinase suppressor of Ras 1	7.9
Gngt2	G protein, gamma transducing activity polypeptide 2	7.8
Uggt1	UDP-glucose glycoprotein glucosyltransferase 1	7.8
Cryab	crystallin, alpha B	7.8
Ang	angiogenin, ribonuclease, RNase A family, 5	7.8
Trex2	three prime repair exonuclease 2	7.8
Zfp295	zinc finger protein 295	7.8
Polrmt	polymerase (RNA) mitochondrial (DNA directed)	7.8
Dnal1	dynein, axonemal, light chain 1	7.8
C1qtnf4	C1q and tumor necrosis factor related protein 4	7.8
Kif26b	kinesin family member 26B	7.7
Hebp1	heme binding protein 1	7.7
Mfn1	mitofusin 1	7.7
Man2a2	mannosidase 2, alpha 2	7.7
Opn3	opsin 3	7.7
Dsn1	DSN1, MIND kinetochore complex component, homolog (S. cerevisiae)	7.6
Npl	N-acetylneuraminatase pyruvate lyase	7.6
Lsr	lipolysis stimulated lipoprotein receptor	7.6
Syndig1	synapse differentiation inducing 1	7.6
Nos1ap	nitric oxide synthase 1 (neuronal) adaptor protein	7.6
Cbln2	cerebellin 2 precursor	7.6
Catsper3	cation channel, sperm associated 3	7.5
Snn	stannin	7.5
Rasa2	RAS p21 protein activator 2	7.5
Wipi2	WD repeat domain, phosphoinositide interacting 2	7.5
Arl5a	ADP-ribosylation factor-like 5A	7.5
P2rx3	purinergic receptor P2X, ligand-gated ion channel, 3	7.5
Tmem132a	transmembrane protein 132A	7.5
Hif1an	hypoxia-inducible factor 1, alpha subunit inhibitor	7.4
Akr1c13	aldo-keto reductase family 1, member C13	7.4
Cav3	caveolin 3	7.4
Ppp1r3b	protein phosphatase 1, regulatory subunit 3B	7.4
Dync2li1	dynein cytoplasmic 2 light intermediate chain 1	7.4
Sord	sorbitol dehydrogenase	7.4
Otud3	OTU domain containing 3	7.4
Car6	carbonic anhydrase 6	7.3
Radil	Ras association and DIL domains	7.3
Layn	layilin	7.3

**Supplementary Table S2** (continued)

Gene Symbol	Description	Fold Change (log2)
Tacc3	transforming, acidic coiled-coil containing protein 3	7.3
Grhl3	grainyhead-like 3 (Drosophila)	7.3
Elf1	E74-like factor 1	7.3
Lrrc4c	leucine rich repeat containing 4C	7.3
Vps4a	vacuolar protein sorting 4 homolog A ( <i>S. cerevisiae</i> )	7.2
Mast3	microtubule associated serine/threonine kinase 3	7.2
RGD1307621	hypothetical LOC314168	7.2
Entpd5	ectonucleoside triphosphate diphosphohydrolase 5	7.2
Pde3b	phosphodiesterase 3B, cGMP-inhibited	7.2
Myh11	myosin, heavy chain 11, smooth muscle	7.1
Synpr	synaptopodin	7.1
Cdc20	cell division cycle 20 homolog ( <i>S. cerevisiae</i> )	7.1
Galnt4	GalNAc-T4	7.1
LOC100188933	hypothetical protein LOC100188933	7.1
Meox2	mesenchyme homeobox 2	7.1
Krt19	keratin 19	7.1
Ints12	integrator complex subunit 12	7.1
RGD1564854	similar to divalent cation tolerant protein CUTA	7.1
Tmem125	transmembrane protein 125	7.1
Scara5	scavenger receptor class A, member 5 (putative)	7.0
Tmem81	transmembrane protein 81	7.0
Bcar3	breast cancer anti-estrogen resistance 3	7.0
Mypn	myopalladin	6.9
Cetn4	centrin 4	6.9
Spc25	SPC25, NDC80 kinetochore complex component, homolog ( <i>S. cerevisiae</i> )	6.9
Atf7	activating transcription factor 7	6.9
Slc30a9	solute carrier family 30 (zinc transporter), member 9	6.9
Zic4	Zic family member 4	6.9
Galnt11	galactosamine:polypeptide N-acetylgalactosaminyltransferase-like 1	6.9
Pigw	phosphatidylinositol glycan anchor biosynthesis, class W	6.9
Gstm5	glutathione S-transferase, mu 5	6.9
Dd25	hypothetical protein Dd25	6.9
St14	suppression of tumorigenicity 14 (colon carcinoma)	6.9
RGD1305014	similar to RIKEN cDNA 2310057M21	6.8
Apbb1ip	A4 precursor protein-binding, family B, member 1 interacting protein	6.8
Haus3	HAUS augmin-like complex, subunit 3	6.8
Serpinf2	serpin peptidase inhibitor, clade F, member 2	6.8
Psmb9	proteasome (prosome, macropain) subunit, beta type 9	6.8
Rsph9	radial spoke head 9 homolog ( <i>Chlamydomonas</i> )	6.8
Pvr12	poliovirus receptor-related 2	6.8
Slc39a8	solute carrier family 39 (zinc transporter), member 8	6.8
Adam4	a disintegrin and metalloprotease domain 4	6.8
Akr1c2	aldo-keto reductase family 1, member C2	6.8
Galnt16	galactosamine:polypeptide N-acetylgalactosaminyltransferase-like 6	6.8
Nedd4l	neural precursor cell expressed, developmentally down-regulated 4-like	6.7
Syncrip	synaptotagmin binding, cytoplasmic RNA interacting protein	6.7
Hyal6	hyaluronoglucosaminidase 6	6.7
Bend6	BEN domain containing 6	6.7
Spag4	sperm associated antigen 4	6.6
Cx3cl1	chemokine (C-X3-C motif) ligand 1	6.6

**Supplementary Table S2** (continued)

Gene Symbol	Description	Fold Change (log2)
Gnb4	guanine nucleotide binding protein (G protein), beta polypeptide 4	6.6
Col23a1	collagen, type XXIII, alpha 1	6.6
Atxn3	ataxin 3	6.6
RGD1563547	RGD1563547	6.6
Rhbd11	rhomboid, veinlet-like 1 ( <i>Drosophila</i> )	6.6
RGD1562726	similar to Putative protein C21orf62 homolog	6.5
Shank1	SH3 and multiple ankyrin repeat domains 1	6.5
Nln	neurolysin (metallopeptidase M3 family)	6.5
Epn3	epsin 3	6.5
Ccdc64	coiled-coil domain containing 64	6.5
Fam186b	family with sequence similarity 186, member B	6.5
Lyl1	lymphoblastic leukemia derived sequence 1	6.5
Rc3h2	ring finger and CCCH-type domains 2	6.4
Nexn	nexilin (F actin binding protein)	6.4
Map3k1	mitogen activated protein kinase kinase kinase 1	6.4
Akt1	v-akt murine thymoma viral oncogene homolog 1	6.4
Tmem171	transmembrane protein 171	6.4
Bpifb1	BPI fold containing family B, member 1	6.4
Tmtc4	transmembrane and tetratricopeptide repeat containing 4	6.4
Ormdl3	ORM1-like 3 ( <i>S. cerevisiae</i> )	6.4
Olr1225	olfactory receptor 1225	6.3
Bcmo1	beta-carotene 15,15'-monooxygenase 1	6.3
Spink2	serine peptidase inhibitor, Kazal type 2 (acrosin-trypsin inhibitor)	6.3
Rassf5	Ras association (RalGDS/AF-6) domain family member 5	6.3
Map4k1	mitogen activated protein kinase kinase kinase kinase 1	6.3
Acads	acyl-CoA dehydrogenase, C-2 to C-3 short chain	6.3
Fcgbp	Fc fragment of IgG binding protein	6.3
Krt8	keratin 8	6.3
Mxd1	max dimerization protein 1	6.2
Cdca8	cell division cycle associated 8	6.2
Efna4	ephrin A4	6.2
RbmX	RNA binding motif protein, X-linked	6.2
Pcdhb9	protocadherin beta 9	6.2
Fkbp11	FK506 binding protein 11	6.2
B3galt4	UDP-Gal:betaGlcNAc beta 1,3-galactosyltransferase, polypeptide 4	6.1
Ppp2r5c	protein phosphatase 2, regulatory subunit B', gamma	6.1
Lyst	lysosomal trafficking regulator	6.1
Zbtb40	zinc finger and BTB domain containing 40	6.1
Pa2g4	proliferation-associated 2G4	6.1
Zbtb8a	zinc finger and BTB domain containing 8a	6.1
Reep1	receptor accessory protein 1	6.1
Actn1	actinin, alpha 1	6.0
Ifih1	interferon induced with helicase C domain 1	6.0
Kctd11	potassium channel tetramerisation domain containing 11	6.0
Rin3	Ras and Rab interactor 3	6.0
Tasp1	taspase, threonine aspartase 1	6.0
Mef2d	myocyte enhancer factor 2D	6.0
Gpx2	glutathione peroxidase 2	6.0
Atp6v1e2	ATPase, H transporting, lysosomal V1 subunit E2	6.0
Usp12	ubiquitin specific peptidase 12	6.0

**Supplementary Table S2** (continued)

Gene Symbol	Description	Fold Change (log2)
Ali3	alpha-1-inhibitor III	6.0
Clgn	calmegin	6.0
Smtn	smoothelin	6.0
Pde7b	phosphodiesterase 7B	5.9
Zbtb38	zinc finger and BTB domain containing 38	5.9
Arrdc2	arrestin domain containing 2	5.9
Lrrc27	leucine rich repeat containing 27	5.9
Rufy2	RUN and FYVE domain containing 2	5.9
Traf3ip1	TNF receptor-associated factor 3 interacting protein 1	5.9
Pex11a	peroxisomal biogenesis factor 11 alpha	5.9
Smpd3	sphingomyelin phosphodiesterase 3, neutral membrane	5.9
Esp11	extra spindle pole bodies homolog 1 (S. cerevisiae)	5.8
Rinl	Ras and Rab interactor-like	5.8
Fam198b	family with sequence similarity 198, member B	5.8
Slc30a1	solute carrier family 30 (zinc transporter), member 1	5.8
Abi3	ABI family, member 3	5.8
Ramp2	receptor (G protein-coupled) activity modifying protein 2	5.8
Exosc2	exosome component 2	5.8
Opn4	opsin 4	5.7
Atf3	activating transcription factor 3	5.7
Evc2	Ellis van Creveld syndrome 2 homolog (human)	5.7
Ang1	angiogenin, ribonuclease A family, member 1	5.7
Mfsd7	major facilitator superfamily domain containing 7	5.7
Lyz16	lysozyme-like 6	5.7
Tbxa2r	thromboxane A2 receptor	5.7
Fam132a	family with sequence similarity 132, member A	5.7
LOC100362783	Uncharacterized protein C7orf61 homolog	5.7
Naalad11	N-acetylated alpha-linked acidic dipeptidase-like 1	5.7
Spa17	sperm autoantigenic protein 17	5.6
Exnef	exonuclease NEF-sp	5.6
Tpk1	thiamin pyrophosphokinase 1	5.6
LOC502684	hypothetical protein LOC502684	5.6
Kif20b	kinesin family member 20B	5.6
Clint1	clathrin interactor 1	5.6
Iah1	isoamyl acetate-hydrolyzing esterase 1 homolog (S. cerevisiae)	5.6
Slc39a12	solute carrier family 39 (zinc transporter), member 12	5.6
Epb49	erythrocyte membrane protein band 4.9 (dematin)	5.6
Ankrd34a	ankyrin repeat domain 34A	5.6
Aoc3	amine oxidase, copper containing 3 (vascular adhesion protein 1)	5.5
Ppp1r1a	protein phosphatase 1, regulatory (inhibitor) subunit 1A	5.5
Polb	polymerase (DNA directed), beta	5.5
Supt7l	suppressor of Ty 7 (S. cerevisiae)-like	5.5
Tg	thyroglobulin	5.5
Cd46	CD46 molecule, complement regulatory protein	5.5
Cntrob	centrobin, centrosomal BRCA2 interacting protein	5.5
Mepe	matrix extracellular phosphoglycoprotein	5.5
Lgals3bp	lectin, galactoside-binding, soluble, 3 binding protein	5.5
Smtnl2	smoothelin-like 2	5.4
Omd	osteomodulin	5.4
Pdhx	pyruvate dehydrogenase complex, component X	5.4